

Syntheses, Thermal Stability, and Structure Determination of the Novel Isostructural $\text{RBa}_3\text{B}_9\text{O}_{18}$ ($\text{R} = \text{Y, Pr, Nd, Sm, Eu, Gd, Tb, Dy, Ho, Er, Tm, Yb}$)

X. Z. Li,[†] C. Wang,[‡] X. L. Chen,^{*†} H. Li,[†] L. S. Jia,[†] L. Wu,[†] Y. X. Du,[†] and Y. P. Xu[†]

Nanoscale Physics and Device Lab, Institute of Physics, Chinese Academy of Sciences, P.O. Box 603, Beijing 100080, People's Republic of China, and Department of Applied Chemistry, Beijing University of Technology, Beijing 100022, People's Republic of China

Received March 6, 2004

A novel borate compound $\text{YBa}_3\text{B}_9\text{O}_{18}$ has crystallized in a melt of $\text{BaYB}_9\text{O}_{16}$. Single-crystal X-ray diffraction measurements reveal that $\text{YBa}_3\text{B}_9\text{O}_{18}$ adopts a hexagonal space group $P6_3/m$ with cell parameters of $a = 7.1761(6)$ Å and $c = 16.9657(6)$ Å. The structure is made up of the planar B_3O_6 groups parallel to each other along the (001) direction, regular YO_6 octahedra, and irregular BaO_6 and BaO_9 polyhedra to form an analogue structure of $\beta\text{-BaB}_2\text{O}_4$. A series of isostructural borate compounds $\text{RBa}_3\text{B}_9\text{O}_{18}$ ($\text{R} = \text{Y, Pr, Nd, Sm, Eu, Gd, Tb, Dy, Ho, Er, Tm, Yb}$) were prepared by powder solid-state reactions. The DTA and TGA curves of $\text{YBa}_3\text{B}_9\text{O}_{18}$ show an obvious weight loss at about 955 °C associated with a decomposition into YBO_3 , B_2O_3 , and $\text{YBa}_3\text{B}_9\text{O}_{18}$ due to its incongruent melting behavior. The DTA and TGA curves of $\text{YBa}_3\text{B}_9\text{O}_{18}$ show that it is chemically stable and a congruent melting compound. A comparison of the structures of $\text{YBa}_3\text{B}_9\text{O}_{18}$ and $\beta\text{-BaB}_2\text{O}_4$ is presented.

Introduction

As part of a search for new materials that could be used as birefringent materials for the manufacturing of optical communication components, such as optical isolators, circulators, and beam displacers, we have investigated the system $\text{Y}_2\text{O}_3\text{--BaO--B}_2\text{O}_3$. The statistics on the minerals indicate that the compounds including Y element probably produce large birefringence. These data also indicate that $[\text{BO}_3]^{3-}$ and $[\text{B}_3\text{O}_6]^{3-}$ that are parallel to each other can produce large birefringence. Polarizations perpendicular to and parallel to the $[\text{BO}_3]^{3-}$ and $[\text{B}_3\text{O}_6]^{3-}$ plane atoms are expected to be very different, just like the $[\text{CO}_3]^{2-}$ in CaCO_3 , to produce large birefringence.^{1,2} With this in mind, we studied the system $\text{Y}_2\text{O}_3\text{--B}_2\text{O}_3\text{--BaO}$ to search for new materials with large birefringence. In the past few years, several new rare-earth (R) and alkaline earth borates such as $\text{RCa}_4\text{O}(\text{B-O}_3)_3$, $\text{R}_2\text{CaO}(\text{BO}_3)_2$, and $\text{RBaB}_9\text{O}_{16}$ have been synthesized.^{3–6}

Among these compounds, the synthesis, structure, and luminescence properties of $\text{RBaB}_9\text{O}_{16}$ have attracted considerable interest as universal hosts of the luminescent materials for tricolor lamps. Consequently, the structure of $\text{RBaB}_9\text{O}_{16}$ and the phase equilibrium diagram around $\text{RBaB}_9\text{O}_{16}$ in the system $\text{R}_2\text{O}_3\text{--BaO--B}_2\text{O}_3$ were studied in a lot of investigations.^{6–8} However, the structure of $\text{RBaB}_9\text{O}_{16}$ is still not fully understood. In this study, we reinvestigate the phase equilibrium relations around $\text{YBaB}_9\text{O}_{16}$ and find the compound $\text{YBaB}_9\text{O}_{16}$ decomposes into $\text{YBa}_3\text{B}_9\text{O}_{18}$, YBO_3 , and B_2O_3 . The new compound of $\text{YBa}_3\text{B}_9\text{O}_{18}$ was discovered, and its structure was determined. The structure is analogous to the structure of $\beta\text{-BaB}_2\text{O}_4$, which has the structural traits for large birefringence discussed above. Its synthesis, its crystal structure, and the comparison of the structures of $\text{YBa}_3\text{B}_9\text{O}_{18}$ and $\beta\text{-BaB}_2\text{O}_4$ are discussed in this paper. Additionally, we discovered a series of isostructural compounds $\text{RBa}_3\text{B}_9\text{O}_{18}$ ($\text{R} = \text{Pr, Nd, Sm, Eu, Gd, Tb, Dy, Ho, Er, Tm, Yb}$).

* To whom correspondence should be addressed. E-mail: xlchen@aphy.iphy.ac.cn.

[†] Chinese Academy of Sciences.

[‡] Beijing University of Technology.

- (1) Wu, L.; Chen, X. L.; Tu, Q. Y.; He, M.; Zhang, Y.; Xu, Y. P. *J. Alloys Compd.* **2002**, *154*, 333.
- (2) Wei, Z. F.; Chen, X. L.; Wang, F. M.; Li, W. C.; He, M.; Zhang, Y. *J. Alloys Compd.* **2001**, *L10*, 327.
- (3) Kuz'micheva, G. M.; Ageev, A. Yu.; Ryhakov, V. B.; Panyutin, V. L.; Yu, Y. M.; Chizhikov, V. I. *Inorg. Mater.* **2001**, *37*, 1051.

- (4) Khamaganova, T. N.; Trunov, V. K.; Kzhurinskii, B. F. *Russ. J. Inorg. Chem.* **1991**, *36*, 484.
- (5) Norrestam, R.; Nygren, M.; Bovin, J. O. *Chem. Mater.* **1992**, *4*, 737.
- (6) Tian, F. W.; Fouassier, C.; Hagenmuller, P. *Mater. Res. Bull.* **1987**, *22*, 389.
- (7) Fu, W. T.; Fouassier, C.; Hagenmuller, P. *Mater Res Bull.* **1987**, *22*, 899.
- (8) Yang, Z.; Lin, J. H.; Su, M. Z.; You, L. P. *Mater. Res. Bull.* **2000**, *35*, 2173.

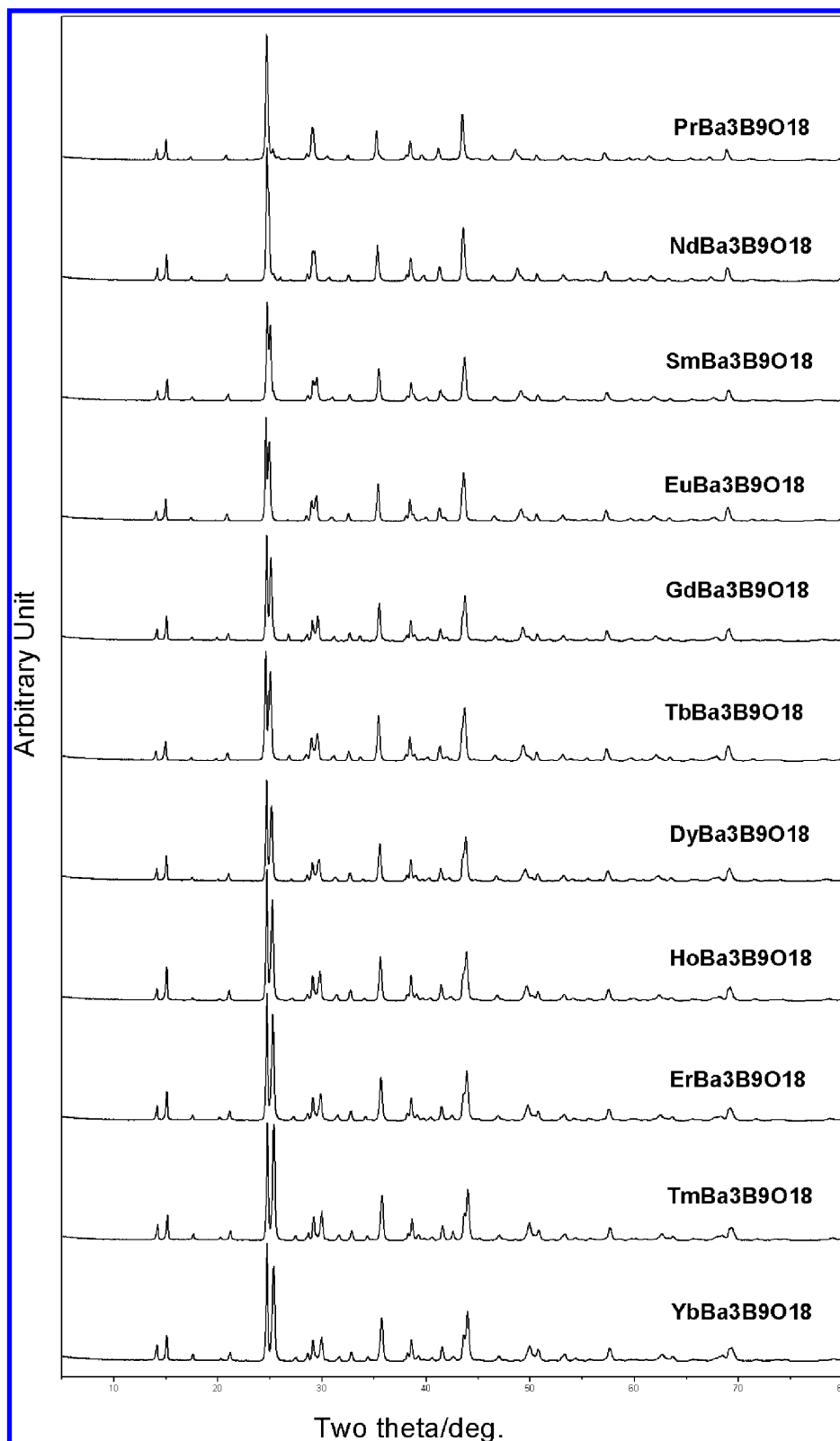


Figure 1. X-ray powder diffraction patterns of $\text{RBa}_3\text{B}_9\text{O}_{18}$ ($\text{R} = \text{Pr}, \text{Nd}, \text{Sm}, \text{Eu}, \text{Gd}, \text{Tb}, \text{Dy}, \text{Ho}, \text{Er}, \text{Tm}, \text{Yb}$).

Experimental Section

Synthesis and Crystal Growth. Single crystals of $\text{YBa}_3\text{B}_9\text{O}_{18}$ were grown by melting the powder of $\text{YBaB}_9\text{O}_{16}$ at a temperature of 1050 °C. A mixture containing appropriate amounts of BaCO_3 (analytical reagent), Y_2O_3 (analytical reagent), and H_3BO_3 (analytical reagent) at molar ratios $\text{Y}/\text{Ba}/\text{B} = 1:1:9$ was ground into fine

powder in a mortar of agate. The mixture was heated to 600 °C in a platinum crucible and kept at this temperature for 12 h, followed by heating at 900 °C for 48 h and at 1050 °C for 4 h to homogenize, then cooled from 1050 to 800 °C at a rate of 1°/h and from 800 to 600 °C at a rate of 2°/h, and finally air-quenched to room temperature. A few colorless crystals of $\text{YBa}_3\text{B}_9\text{O}_{18}$ were found at

Table 1. Experimental Details of Single-Crystal Data Collection and Refinement

molecular formula	$\text{YBa}_3\text{B}_9\text{O}_{18}$
molecular wt	886.2
cryst syst	hexagonal
space group	$P6_3/m$
unit cell dimensions/Å	$a = 7.1766(9), c = 16.9657(21)$
$V/\text{Å}^3$	756.1(1)
Z	2
density (calcd)/ gcm^{-3}	3.89
μ/mm^{-1}	11.60
color	colorless
diffractometer	Bruker SMART APEX CCD area-detector diffractometer
radiation, temperature/K	$\text{Mo K}\alpha$, 293(2)
wavelength/Å	0.71073
abs correction	SADABS, Bruker/Siemens area detector absorption and other corrections, V2.03
reflns for refined cell params	3281
scan mode	φ and ω scans
measured reflns	7192
indep reflns with $I > 2\sigma(I)$	1920
data collection range/deg	$6.552 < 2\theta < 66.983$
index ranges	$-10 \leq h \leq 10,$ $-10 \leq k \leq 11,$ $-16 \leq l \leq 26$
reflns used in the last refinement	1006
weighting scheme	$w = 1/[\sigma^2(F_o^2) + (0.0330)^2 + 22.75P]$ where $P = (F_o^2 + 2F_c^2)/3$
no. refined params	70
reliability factor	0.0568, 0.1323
R_1, wR_2 (all data)	
GOF	1.170

Table 2. Selected Interatomic Distances (Å) and Angles (deg) in $\text{YBa}_3\text{B}_9\text{O}_{18}^a$

Ba(1)–O(3)	2.714(4)	Y(1)–O(4) _{iv,vii,viii,ix,x}	2.252(5)
Ba(1)–O(3) _{ii}	2.714(4)	Y(1)–O(4)	2.252(5)
Ba(1)–O(4) _{iii,iv,v}	2.888(5)	Ba(2)–O(3) _{ii,xi,xii}	2.713(7)
Ba(1)–O(2)	2.988(5)	Ba(2)–O(1) _{xiii,iv}	2.879(7)
Ba(1)–O(2) _{i,vi}	2.988(5)	Ba(2)–O(1)	2.879(7)
B(1)–O(3)	1.303(12)	O(1)–B(1)–O(3)	124.1(9)
B(1)–O(1)	1.395(13)	O(1) _{xiv} –B(1)–O(3)	120.0(9)
B(1)–O(1) _{xiv}	1.417(13)	O(1) _{xiv} –B(1)–O(1)	116.0(9)
B(2)–O(4)	1.319(8)	O(2) _{ix} –B(2)–O(4)	120.3(6)
B(2)–O(2) _{ix}	1.400(8)	O(2) _{xii} –B(2)–O(4)	122.9(6)
B(2)–O(2) _{xii}	1.400(9)	O(2) _{ix} –B(2)–O(2) _{xii}	116.7(6)

^a Symmetry codes: (i) $-y + 1, x - y, z$; (ii) $-x + y + 1, -x + 1, -z + 1/2$; (iii) $-x + y + 1, -x, z$; (iv) $-y, x - y, z$; (v) $x + 1, y + 1, z$; (vi) $-x + y + 1, -x + 1, z$; (vii) $x - y, x, -z$; (viii) $-x, -y, -z$; (ix) $-x + y, -x, z$; (x) $y, -x + y, -z$; (xi) $-y, x - y - 1, z$; (xii) $x - 1, y, z$; (xiii) $-x + y, -x, -z + 1/2$; (xiv) $-x + y + 1, -x, -z + 1/2$.

the wall of the platinum crucible from the melt, and the white YBO_3 , $\text{YBa}_3\text{B}_9\text{O}_{18}$, and $\text{YBaB}_9\text{O}_{16}$ were found at the bottom of the platinum crucible. We studied the phase equilibrium diagram around $\text{YBaB}_9\text{O}_{16}$ by using the solid-state reactions. Samples of $\text{YBa}_3\text{B}_9\text{O}_{18}$ were prepared from reagent-grade mixtures of BaCO_3 , Y_2O_3 , and H_3BO_3 at molar ratios $\text{Y}/\text{Ba}/\text{B} = 1:3:9$. These mixtures were heated in a mortar of agate to 930 °C for 48 h.

The $\text{RBa}_3\text{B}_9\text{O}_{18}$ ($R = \text{La, Ce, Y, Pr, Nd, Sm, Eu, Gd, Tb, Dy, Ho, Er, Tm, Yb}$) compounds were readily synthesized from stoichiometric mixtures of BaCO_3 (analytical reagent), R_2O_3 ($R = \text{La, Nd, Sm, Eu, Gd, Dy, Ho, Er, Tm, Yb}$ (analytical reagent)), CeO_2 , Tb_4O_7 , and H_3BO_3 (analytical reagent) powders. The mixtures were heated to 800–930 °C in air for 2–3 days, and the purity of the products was checked by powder X-ray diffraction using an X-ray diffractometer (MXP21VAHF/M21X, MAC Science) with a power of 40 kV at 250 mA, employing $\text{Cu K}\alpha$ radiation by using a graphite monochromator. In the case of $R = \text{La}$ and Ce , the reaction did not result in a compound isostructural to $\text{RBa}_3\text{B}_9\text{O}_{18}$ ($R = \text{Y, Pr, Nd, Sm, Eu, Gd, Tb, Dy, Ho, Er, Tm, Yb}$) probably because the ionic radius of La^{3+} , Ce^{4+} is too large. The X-ray powder diffraction

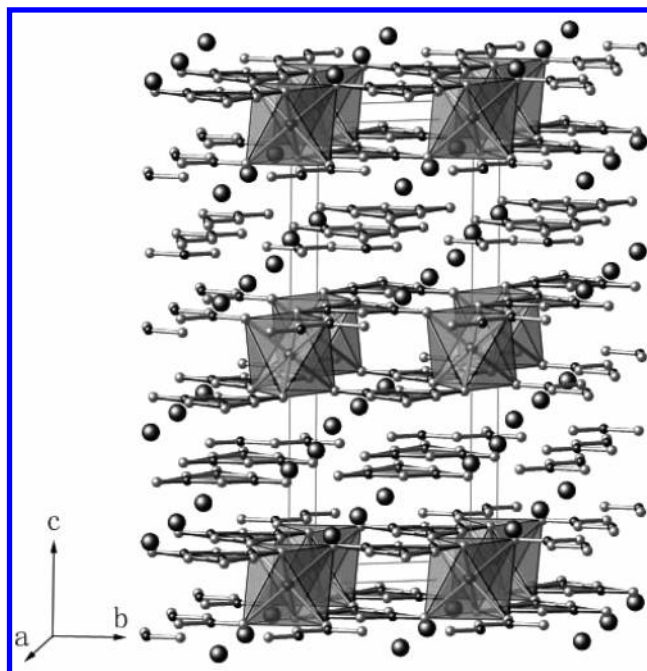


Figure 2. Structure of $\text{YBa}_3\text{B}_9\text{O}_{18}$. Large black circles stand for Ba atoms, octahedra stand for YO_6 polyhedra, and gray planar polyhedra stand for $[\text{B}_3\text{O}_6]^{3-}$ triangles in which small black circles stand for B atoms and gray ones stand for O atoms.

patterns of $\text{RBa}_3\text{B}_9\text{O}_{18}$ ($R = \text{Pr, Nd, Sm, Eu, Gd, Tb, Dy, Ho, Er, Tm, Yb}$) were taken at room temperature in the step scan mode, at a step value of 0.02° , measuring for 3 s at each step. For $\text{RBa}_3\text{B}_9\text{O}_{18}$ ($R = \text{Pr, Nd, Sm, Eu, Gd, Tb, Dy, Ho, Er, Tm, Yb}$), the powder X-ray diffraction patterns are seen in Figure 1.

Single-Crystal X-ray Crystallography. A single crystal of $\text{YBa}_3\text{B}_9\text{O}_{18}$ with approximate dimensions $0.1 \times 0.08 \times 0.05 \text{ mm}^3$ was selected for single-crystal X-ray diffraction. The diffraction data of $\text{YBa}_3\text{B}_9\text{O}_{18}$ were collected on a Bruker SMART APEX CCD area-detector diffractometer with graphite monochromator and $\text{Mo K}\alpha$ radiation. Cell constants were obtained from least-squares refinement in the hexagonal space group $P6_3/m$, using the setting angles of 3281 reflections in the range $6.552 < 2\theta < 66.983$. The structure of $\text{YBa}_3\text{B}_9\text{O}_{18}$ was solved by direct method and Fourier synthesis using the SHELX-97 software.⁹ The experimental details and crystallographic parameters are given in Table 1. Selected bond lengths and angles are listed in Table 2.

Element Content Determination. The Y, Ba, and B contents in the crystal were determined by using ICP-6500 plasma spectrometer.

IR Spectra Measurements. Infrared spectra were recorded with a Perkin-Elmer 983 infrared spectrophotometer in the 200–2000 cm^{-1} wavenumber range using KBr pellets.

Differential Thermal Analysis. The melting behaviors of $\text{YBaB}_9\text{O}_{16}$ and $\text{YBa}_3\text{B}_9\text{O}_{18}$ were investigated by differential thermal analysis (DTA). A DTA measurement was carried out with a CP-G high-temperature differential thermal instrument. The precision of measurement was $\pm 3^\circ\text{C}$. The heating rate was $10^\circ\text{C}/\text{min}$ from room temperature to 1200 °C.

Results and Discussion

Description of the $\text{YBa}_3\text{B}_9\text{O}_{18}$ Structure. The $\text{YBa}_3\text{B}_9\text{O}_{18}$ compound crystallizes with a novel structure type. As

(9) Sheldrick, G. M. *SHELXS97 and SHELXL97*; University of Göttingen: Göttingen, Germany, 1997.

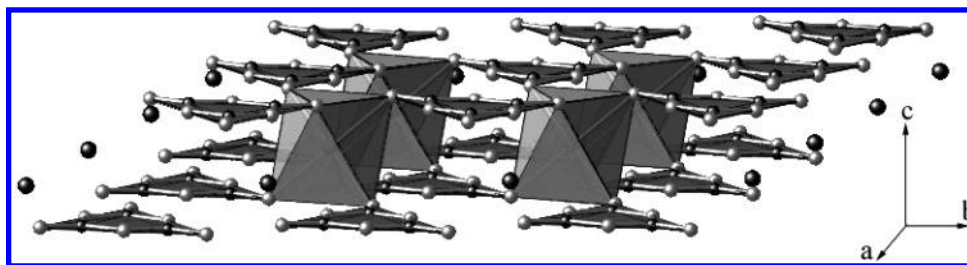


Figure 3. View of the structure formed by YO_6 and B_3O_6 polyhedra.

illustrated in Figure 2, the fundamental building unit of $\text{YBa}_3\text{B}_9\text{O}_{18}$ structure is the planar B_3O_6 group. The planar B_3O_6 groups are parallel to each other and distributed layer upon layer along the c -axis. Y atoms occupy sites between the B_3O_6 sheets and are bonded to 6 oxygen atoms, each belonging to a different B_3O_6 group. As a result, regular octahedra are formed with an equal $\text{Y}-\text{O}$ bond length of $2.252(5)\text{\AA}$. Six vertexes of each YO_6 octahedron interconnect six planar B_3O_6 groups, and three vertexes of each planar B_3O_6 group interconnect three YO_6 octahedra, as shown in Figure 3. In this structure, five kinds of coordination with oxygen are present: regular $\text{YO}(4)_6$ octahedra, distorted $\text{Ba}(1)\text{O}_6$ hexagon, irregular $\text{Ba}(2)\text{O}_9$ polyhedra, and two types of planar B_3O_6 groups. The 18 borate anions in the unit cell of the $\text{YBa}_3\text{B}_9\text{O}_{18}$ structure are found to divide into two sets. In the larger set at the (12i) position, three B(2) with three O(2) and three O(4) at the (12i) position form B_3O_6 groups which interconnect $\text{YO}(4)_6$ octahedra and irregular $\text{Ba}(2)\text{O}_9$ parallel to the ab crystal plane. In the smaller set at (6h) position, B1 species are coordinated to O(1) and O(3) at the (6h) position to form B_3O_6 groups. The three vertexes O(3) of B_3O_6 triangle share with two $\text{Ba}(2)\text{O}_9$ and one $\text{Ba}(1)\text{O}_6$, and the three O(1) at the edge of B_3O_6 triangle are common with three planar $\text{Ba}(1)\text{O}_6$, as shown in Figure 4.

In order to further confirm the coordination surroundings of B–O in the $\text{YBa}_3\text{B}_9\text{O}_{18}$ structure, the IR spectrum of $\text{YBa}_3\text{B}_9\text{O}_{18}$ was measured at room temperature and given in Figure 5. Bands below 400 cm^{-1} should be due to crystal lattice vibrations. The IR absorption at wavenumbers smaller than 800 cm^{-1} originates mainly from the lattice dynamic modes and will not be considered due to its complexity. According to previous work,¹⁰ the strong bands above 1200 cm^{-1} should be assigned to the triangular B_3O_6 groups.

To examine the validity of the determined structure, Brown's bond valence theory¹¹ was used to calculate the valence sum for the ions. The results of the calculations are given in Table 3. We can see that the calculated valence sums are in good agreement with their normal valences.

Isostructural Compounds $\text{R}\text{Ba}_3\text{B}_9\text{O}_{18}$ ($\text{R} = \text{Y, Pr, Nd, Sm, Eu, Gd, Tb, Dy, Ho, Er, Tm, Yb}$). The powder diffraction data of the compounds $\text{R}\text{Ba}_3\text{B}_9\text{O}_{18}$ ($\text{R} = \text{Pr, Nd, Sm, Eu, Gd, Tb, Dy, Ho, Er, Tm, Yb}$) can be indexed on the basis of a hexagonal cell using the Dicol91 program.¹² Their lattice parameters, volume, and figure-of-merit ($M(25)$,

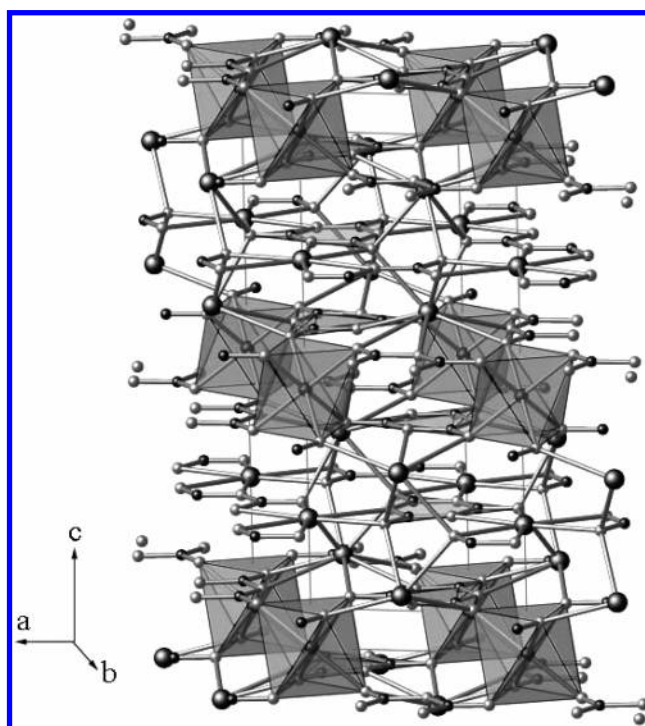


Figure 4. View of the structure formed by BaO_6 , BaO_9 , and B_3O_6 polyhedra.

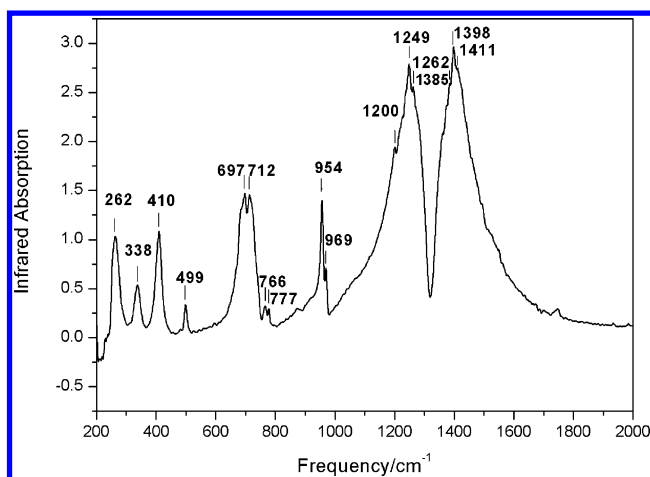


Figure 5. Infrared spectra of $\text{YBa}_3\text{B}_9\text{O}_{18}$.

$F(25)$) are given in Table 4. We can see that the lattice parameters and the volume of $\text{R}\text{Ba}_3\text{B}_9\text{O}_{18}$ ($\text{R} = \text{Pr, Nd, Sm, Eu, Gd, Tb, Dy, Ho, Er, Tm, Yb}$) decrease with the decreasing of the radius of R. From the variation of their lattice parameters and the conditions on the systematic extinction, we can judge that these compounds are isostructural to $\text{YBa}_3\text{B}_9\text{O}_{18}$.

(10) Nakamoto, K. *Infrared Spectra of Inorganic and Coordination Compounds*; Wiley: New York, 1963.

(11) Brown, I. D.; Altermatt, D. *Acta Crystallogr., Sect. B* **1985**, *41*, 244.

(12) Boulif, A.; Louer, D. *J. Appl. Crystallogr.* **1991**, *24*, 987.

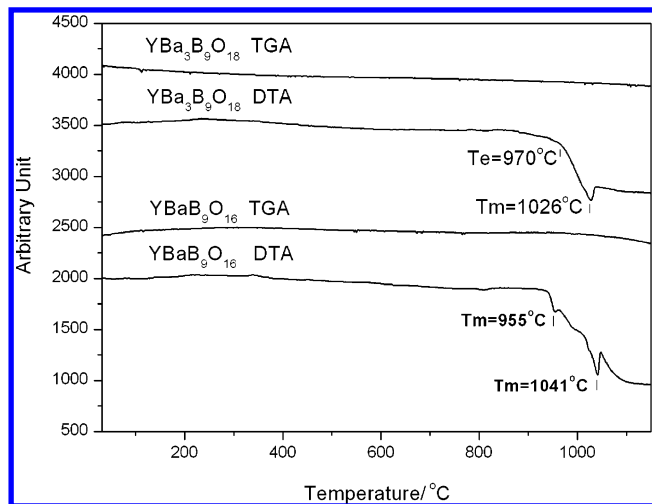


Figure 6. DTA and TGA curves of $YBaB_9O_{16}$ and $YBa_3B_9O_{18}$.

Table 3. Ba–O, Y–O, and B–O Bond Valence in $YBa_3B_9O_{18}$

	O1	O2	O3	O4	Σ_s
Ba1		0.150 × 3	0.314 × 3	0.196 × 3	1.980
Ba2	0.249 × 3		0.326 × 3		1.725
Y1				0.531 × 6	3.186
B1	0.947		1.199		3.024
	0.878				
B2		0.927		1.151	3.000
		0.922			
Σ_s	2.074	1.999	1.839	1.878	

Thermal Stability. Figure 6 presents the DTA and TGA curves of $YBaB_9O_{16}$ and $YBa_3B_9O_{18}$, respectively. The TGA curve of $YBaB_9O_{16}$ indicates an obvious weight loss at about 940 °C associated with the decomposition into YBO_3 , $YBa_3B_9O_{18}$, and B_2O_3 due to incongruent melting behavior. The peak at about 1019 °C should be the melting point of

Table 4. The Lattice Parameters and Figure-of-Merit of the Isostructural Compounds $RBa_3B_9O_{18}$ (R = Pr, Nd, Sm, Eu, Gd, Tb, Dy, Ho, Er, Tm, Yb)

	$a/\text{Å}$	$c/\text{Å}$	$V/\text{Å}^3$	$M(2\theta)$	$F(2\theta)$
Pr $Ba_3B_9O_{18}$	7.2035(6)	17.534(3)	787.971	28.7	22.7
Nd $Ba_3B_9O_{18}$	7.2026(6)	17.439(3)	783.550	29.7	22.5
Sm $Ba_3B_9O_{18}$	7.1980(5)	17.336(3)	777.298	33.0	32.6
Eu $Ba_3B_9O_{18}$	7.1960(7)	17.265(2)	774.263	35.7	34.9
Gd $Ba_3B_9O_{18}$	7.1934(6)	17.206(3)	771.040	41.9	54.5
Tb $Ba_3B_9O_{18}$	7.1884(6)	17.155(3)	767.690	39.8	48.2
Dy $Ba_3B_9O_{18}$	7.1843(7)	17.106(2)	764.652	35.5	51.3
Ho $Ba_3B_9O_{18}$	7.1833(6)	17.047(2)	761.833	43.2	56.4
Er $Ba_3B_9O_{18}$	7.1817(6)	16.996(2)	759.180	37.8	48.7
Tm $Ba_3B_9O_{18}$	7.1780(4)	16.959(1)	756.745	51.7	68.0
Yb $Ba_3B_9O_{18}$	7.1740(5)	16.915(2)	753.972	50.6	67.7

the compound $YBa_3B_9O_{18}$. The sample after the DTA experiments was found to be a mixture of YBO_3 (white powder in the bottom of platinum crucible) and a highly volatile glass phase of $YBa_3B_9O_{18}$ and B_2O_3 . We first find the $YBa_3B_9O_{18}$ compound and correct the phase equilibrium diagram in the B_2O_3 rich part of the Y_2O_3 – BaO – B_2O_3 system as shown in Figure 7. The DTA and TGA curves of $YBa_3B_9O_{18}$ show that it is chemically stable and a congruent melting compound, which suggests that the crystal of $YBa_3B_9O_{18}$ can be easily grown. The chemical analyses for single crystals indicate that the composition of the compound is $YBa_3B_9O_{18}$, which is consistent with nominal composition of the powder sample.

Comparison of the Structures of $YBa_3B_9O_{18}$ and β - BaB_2O_4 . The possible reason the compounds $RBa_3B_9O_{18}$ (R = Y, Pr, Nd, Sm, Eu, Gd, Tb, Dy, Ho, Er, Tm, Yb) were not been found in previous investigations is that its diffraction pattern is very similar to that of β - BaB_2O_4 . In comparison with their powder X-ray patterns, we can see that the stronger

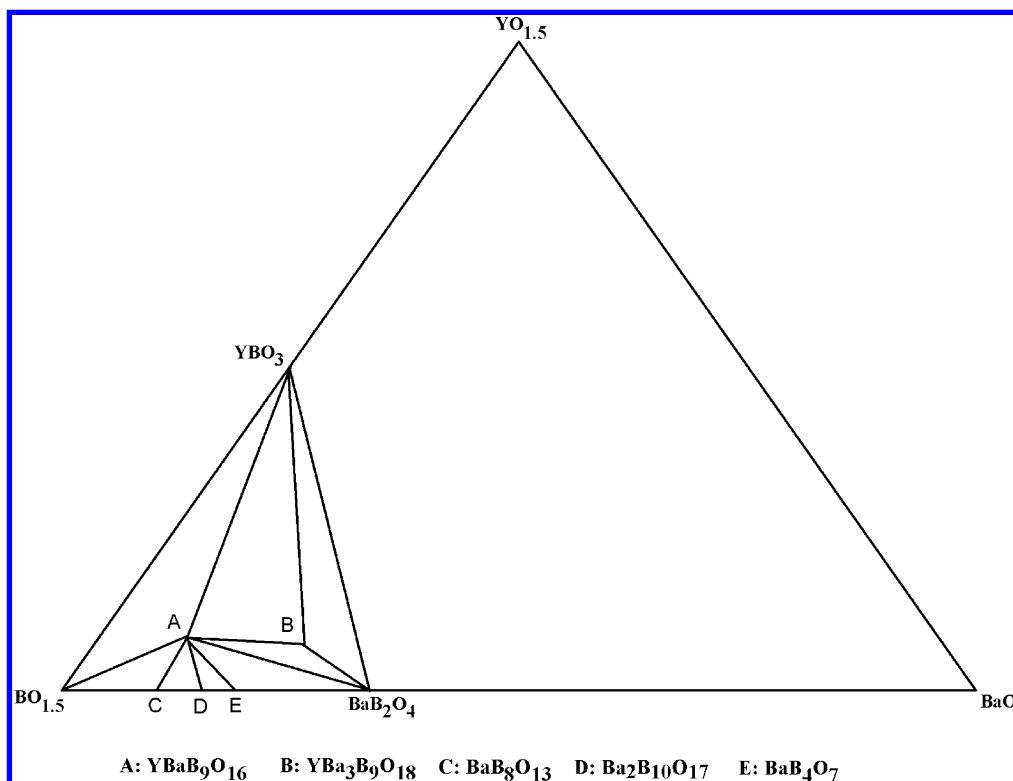
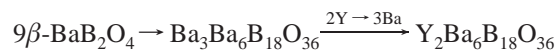


Figure 7. Subsolidus phase relation in the BaB_2O_4 – YBO_3 – B_2O_3 system.

lines in the XRD of $\text{RBA}_3\text{B}_9\text{O}_{18}$ ($\text{R} = \text{Y}, \text{Pr}, \text{Nd}, \text{Sm}, \text{Eu}, \text{Gd}, \text{Tb}, \text{Dy}, \text{Ho}, \text{Er}, \text{Tm}, \text{Yb}$) and $\beta\text{-BaB}_2\text{O}_4$ overlap each other. By comparison, the compounds $\text{RBA}_3\text{B}_9\text{O}_{18}$ ($\text{R} = \text{Y}, \text{Pr}, \text{Nd}, \text{Sm}, \text{Eu}, \text{Gd}, \text{Tb}, \text{Dy}, \text{Ho}, \text{Er}, \text{Tm}, \text{Yb}$) are considered to form by replacing 3Ba by 2Y in $9\beta\text{-BaB}_2\text{O}_4$ ($\text{Ba}_9\text{B}_{18}\text{O}_{36}$). This reaction can be shown by the following formula:



In $\text{YBa}_3\text{B}_9\text{O}_{18}$, 3Ba substituted by 2Y makes $\text{YBa}_3\text{B}_9\text{O}_{18}$ stable and prevents the phase transition. $\text{YBa}_3\text{B}_9\text{O}_{18}$ keeps the structural traits of B_3O_6 groups in $\beta\text{-BaB}_2\text{O}_4$ and makes the Y and Ba atoms rearrange. From the structures of $\text{YBa}_3\text{B}_9\text{O}_{18}$ and $\beta\text{-BaB}_2\text{O}_4$, we can see that their structures have many similar structural traits and transform into each other possibly. The differences between them is that $\text{YBa}_3\text{B}_9\text{O}_{18}$ has higher symmetry than $\beta\text{-BaB}_2\text{O}_4$ and the B_3O_6 groups are much flatter than that in $\beta\text{-BaB}_2\text{O}_4$.

In conclusion, a novel series of isostructural borates of

rare earth and barium compounds $\text{RBA}_3\text{B}_9\text{O}_{18}$ ($\text{R} = \text{Y}, \text{Pr}, \text{Nd}, \text{Sm}, \text{Eu}, \text{Gd}, \text{Tb}, \text{Dy}, \text{Ho}, \text{Er}, \text{Tm}, \text{Yb}$) have been synthesized, and the crystal structures and the thermal stability have been studied. The structures of $\text{RBA}_3\text{B}_9\text{O}_{18}$ ($\text{R} = \text{Y}, \text{Pr}, \text{Nd}, \text{Sm}, \text{Eu}, \text{Gd}, \text{Tb}, \text{Dy}, \text{Ho}, \text{Er}, \text{Tm}, \text{Yb}$) are similar to that of $\beta\text{-BaB}_2\text{O}_4$. The difference between them is that in $\text{RBA}_3\text{B}_9\text{O}_{18}$ ($\text{R} = \text{Y}, \text{Pr}, \text{Nd}, \text{Sm}, \text{Eu}, \text{Gd}, \text{Tb}, \text{Dy}, \text{Ho}, \text{Er}, \text{Tm}, \text{Yb}$) the yttrium atom at the 2b site is made up of regular octahedra and the B_3O_6 group is much flatter than that in $\beta\text{-BaB}_2\text{O}_4$.

Acknowledgment. This work was financially supported by the National Natural Science Foundation of China (under the Grants 50102009 and 50372081) and the International Centre for Diffraction Data.

Supporting Information Available: Crystallographic data in CIF format. This material is available free of charge via the Internet at <http://pubs.acs.org>.

IC049710M